

Elliptic flow of transported and produced protons in Au+Au collisions with the UrQMD model

Biao Tu, Shusu Shi,^{*} and Feng Liu[†]

*Key Laboratory of Quarks and Lepton Physics (MOE) and Institute of Particle Physics,
Central China Normal University, Wuhan, 430079, China*

With the framework of the UrQMD model, by tracing the number of initial quarks in protons, we study the elliptic flow of protons with 3, 2, 1, 0 initial quarks and anti-protons in Au+Au collisions at $\sqrt{s_{NN}} = 7.7, 11.5, 39, 200$ GeV. The difference of elliptic flow between protons with 2, 1, 0 initial quarks and anti-protons is smaller than 0 or consistent with 0, respectively. The difference of elliptic flow between transported protons (with 3 initial quarks) and anti-protons is larger than 0 at 7.7, 11.5 and 39 GeV. It shows a good agreement with the STAR results at 7.7 and 11.5 GeV, but overestimates the STAR results at 39 GeV. The yield of transported protons with 3 initial quarks is smaller than that of protons with 2 and 1 initial quarks and the v_2 of all protons is much smaller than the STAR results. The observation of the difference of elliptic flow between transported protons and anti-protons in the UrQMD model partly explains the v_2 difference between protons and anti-protons observed in the Beam Energy Scan program in Relativistic Heavy Ion Collider (RHIC).

I. INTRODUCTION

A strongly interacting hot and dense QCD matter called quark-gluon plasma (QGP) is created in the experiments of high-energy heavy-ion collisions at the Relativistic Heavy Ion Collider (RHIC) and the Large Hadron Collider (LHC) [1–6]. To understand the properties and phase structure of strongly interacting nuclear matter, the Beam Energy Scan (BES) program involving Au+Au collisions has been carried out at RHIC. Various observables have been measured such as particle production and ratios [7, 8], Hanbury-Brown-Twiss (HBT) interferometry [9], moments of the conserved quantities [10] and collective flow [11]. In this paper, we focus on the second harmonic of collective flow, v_2 . Analyzing the anisotropic flow in nucleus-nucleus collisions is one of the most important directions in studying the properties of created matter [12–14], since it is sensitive to the pressure gradient, degree of freedom, equation of state (EoS) [15, 16] and degree of thermalization in the early stages of nuclear collisions.

Some interesting phenomena have been observed in heavy-ion collisions of the BES program. The smaller v_2 of \bar{p} , K^- and π^+ than those of p , K^+ and π^- , are observed respectively. The v_2 difference decreases with increasing colliding energy [17–21]. These interesting results were attributed to the different v_2 of transported and produced quarks during the initial stage of heavy-ion collisions in ref. [22]. It is argued that the effect results from quark transportation from forward to middle rapidity. The authors assume that the v_2 of transported quarks is larger than that of produced quarks. Thus, the different numbers of constituent quarks and anti-quarks in the particles and corresponding antiparticles lead to a systematically larger v_2 of the baryons compared to the

anti-baryons. The energy dependence is explained by the increase of nuclear stopping in heavy-ion collisions with decreasing colliding energy [23]. In ref. [24], it is suggested that the chiral magnetic effect induced by the strong magnetic field in noncentral collisions could be responsible for the observed difference between the v_2 of π^+ and π^- .

A calculation [25, 26] based on the Nambu-Jona-Lasinio (NJL) model can also qualitatively explain the difference between $p - \bar{p}$, $\Lambda - \bar{\Lambda}$ and $K^+ - K^-$ by incorporating repulsive potential for quarks and attractive potential for antiquarks, which results in different flow patterns. The other study [27] based on the AMPT model including mean-field potential can also qualitatively explain the difference between the elliptic flow of particles and their corresponding antiparticles. Because of the more attractive potentials of \bar{p} compared to p , smaller v_2 is obtained for \bar{p} . With the attractive K^- and repulsive K^+ potentials, and slightly attractive π^+ and repulsive π^- potentials, smaller v_2 are obtained for K^- and π^+ than that of K^+ and π^- .

In this paper, we study the elliptic flows of protons with 3 initial quarks, 2 initial quarks, 1 initial quark, 0 initial quark and anti-protons at BES energies with a ultra relativistic quantum molecular dynamics (UrQMD) model [28, 29]. The paper is organized as follows: in section II, the observable is introduced. A brief description of the UrQMD model is given in section III. The results and discussions are presented in section IV. Finally, a summary is given in section V.

II. OBSERVABLE

The azimuthal anisotropy is one of the most important observables in heavy-ion collisions. In the non-central heavy-ion collisions, the overlap region is an almond shape with the major axis perpendicular to the reaction plane which is defined by the impact parameter

^{*} shiss@mail.cnu.edu.cn

[†] fliu@mail.cnu.edu.cn

and the beam direction. As the system evolves, the pressure gradient from the overlapping region of two nuclei in the collisions is the origin of the collective motion component in mid-rapidity. The anisotropy in the coordinate space is transferred to the anisotropy in the momentum space. The anisotropic parameters are defined by the Fourier coefficients of the expansion of the azimuthal distribution [30, 31] of the produced particles with respect to the reaction plane which can be written as

$$E \frac{d^3 N}{dp^3} = \frac{1}{2\pi} \frac{d^2 N}{p_T dp_T dy} (1 + 2 \sum v_n \cos[n(\phi - \Psi_{\text{RP}})]) \quad (1)$$

where ϕ is the azimuthal angle of the particles. Ψ_{RP} is the reaction plane. The anisotropic parameter is defined as the n^{th} Fourier coefficient v_n :

$$v_n = \langle \cos[n(\phi - \Psi_{\text{RP}})] \rangle, \quad (2)$$

where $\langle \dots \rangle$ is taking the average over all the particles in the sample. The second harmonic coefficient is denoted as elliptic flow v_2 . In the UrQMD model, Ψ_{RP} is fixed at zero degree.

III. URQMD MODEL

The ultrarelativistic quantum molecular dynamics (UrQMD) model is a microscopic transport model which could simulate the $p + p$, $p + A$, and $A + A$ collisions at relativistic energies and describes the time-evolution of a many-body system by using covariant equations of motion. It includes the string excitation and fragmentation, the formation and decay of hadronic resonances, and rescattering of hadrons. At low and intermediate energies, this microscopic transport model focuses on the interactions between known baryon and meson species and their resonances. The excitation and fragmentation of color strings play important roles in the particle production at high energies in the UrQMD model. The version of the UrQMD model we used in this article is 2.3, and no modification was made to the model itself except for some additional outputs for tracing the particle's origin as explained in ref [32]. We marked particles as transported and produced by tracing the number of initial quarks in a particle. In this article, protons with 3, 2, 1 and 0 initial quark are marked as $p(3 \text{ iq})$, $p(2 \text{ iq})$, $p(1 \text{ iq})$ and $p(0 \text{ iq})$ respectively. There are two special cases. Protons with three initial quarks are treated as transported protons($p(3 \text{ iq})$). Protons with zero initial quark are treated as produced protons($p(0 \text{ iq})$). Produced protons and anti-protons are both made of three produced quarks, thus they are expected to be similar in many aspects.

IV. RESULTS AND DISCUSSIONS

By tracing the number of initial quarks in proton, the $p(3 \text{ iq})$ account for 17.4% at 7.7 GeV, 8.3% at 11.5 GeV,

1.26% at 39 GeV and 0.36% at 200 GeV of all protons and anti-protons in the middle rapidity ($|Y| < 1$). The $p(2 \text{ iq})$ account for 80.8% at 7.7 GeV, 84% at 11.5 GeV, 52.83% at 39 GeV and 10.9% at 200 GeV. The $p(1 \text{ iq})$ account for 0.91% at 7.7 GeV, 3% at 11.5 GeV, 12.46% at 39 GeV and 14.4% at 200 GeV. The $p(0 \text{ iq})$ account for 0.45% at 7.7 GeV, 2.4% at 11.5 GeV, 15.4% at 39 GeV and 39.1% at 200 GeV. The \bar{p} account for 0.44% at 7.7 GeV, 2.3% at 11.5 GeV, 18.05% at 39 GeV and 35.24% at 200 GeV. The upper panel of Figure 1 shows the elliptic flow of $p(3 \text{ iq})$, $p(2 \text{ iq})$, $p(1 \text{ iq})$, $p(0 \text{ iq})$ and \bar{p} within $0.2 < p_T < 2.0 \text{ GeV}/c$ as a function of collision centrality in Au+Au collisions at various colliding energies. One can find that v_2 shows strong centrality dependence since it is mainly driven by the initial spatial eccentricity. The lower panel shows the difference of v_2 between $p(3 \text{ iq})$, $p(2 \text{ iq})$, $p(1 \text{ iq})$, $p(0 \text{ iq})$ and \bar{p} , respectively. The difference of v_2 between $p(0 \text{ iq})$ (produced) and \bar{p} does not show clearly centrality dependence, and is approximately consistent with 0. As we mentioned above, the $p(0 \text{ iq})$ should be similar to \bar{p} in many aspects. They are all made up by produced quarks. The $p(0 \text{ iq})$ and \bar{p} both are produced at the early stage of the system that energy density is relatively large in low colliding energies. Both $p(0 \text{ iq})$ and \bar{p} experience the full evolution of the system which lead to a similar magnitude of v_2 . Larger elliptic flow of $p(3 \text{ iq})$ than that of $p(0 \text{ iq})$ and \bar{p} is observed. It suggests the v_2 of $p(3 \text{ iq})$ transported from forward rapidity to mid-rapidity due to nuclear stopping effect is different from the v_2 of $p(0 \text{ iq})$ and \bar{p} . These results indicate that the elliptic flow of transported quarks is larger than that of produced quarks. The transported quarks which have been transported over a large rapidity suffer more scatterings than the produced quarks. It develops a larger v_2 of transported quarks than that of produced quarks, thus can lead to a larger v_2 of $p(3 \text{ iq})$ than that of $p(0 \text{ iq})$. The difference of v_2 between $p(3 \text{ iq})$ and \bar{p} shows a strong centrality dependence. Larger difference is observed in middle central collisions than that in most central and peripheral collisions at 7.7, 11.5 and 39 GeV. The $p(3 \text{ iq})$ experiences the whole process that the initial geometry eccentricity is transformed into anisotropy in the momentum space, whereas the $p(0 \text{ iq})$ may only partly experiences the process. The combination of baryon stopping effect and scatterings makes the difference of v_2 between the transported protons and anti-protons largest in mid-central collisions. No significant centrality dependence is observed at 200 GeV due to the small difference of v_2 between $p(3 \text{ iq})$ and \bar{p} .

The v_2 of $p(2 \text{ iq})$ and $p(1 \text{ iq})$ show similar centrality dependence with that of v_2 of $p(0 \text{ iq})$ and \bar{p} , but are systematically lower than the v_2 of $p(0 \text{ iq})$ and \bar{p} . The $p(0 \text{ iq})$, $p(1 \text{ iq})$, $p(2 \text{ iq})$ and \bar{p} are produced at the same time at early stage based on a string-excitation scheme [32], but part of $p(1 \text{ iq})$ and $p(2 \text{ iq})$ are produced by the decay of unstable baryons. It means the formation time of $p(0 \text{ iq})$ and \bar{p} should be earlier than that of $p(1 \text{ iq})$ and $p(2 \text{ iq})$. So $p(1 \text{ iq})$ and $p(2 \text{ iq})$ suffer less interactions than

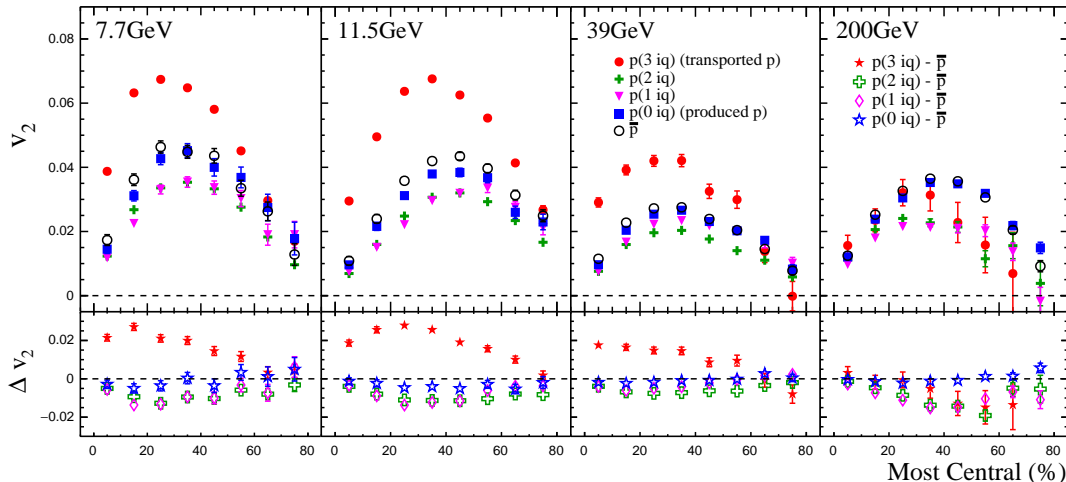


FIG. 1: (Color online) Upper panel: The elliptic flow of $p(3 \text{ iq})$, $p(2 \text{ iq})$, $p(1 \text{ iq})$, $p(0 \text{ iq})$ and \bar{p} are plotted as a function of collision centrality in Au+Au collisions at $\sqrt{s_{NN}} = 7.7, 11.5, 39, 200$ GeV. Lower panel: The difference of v_2 between $p(3 \text{ iq})$, $p(2 \text{ iq})$, $p(1 \text{ iq})$, $p(0 \text{ iq})$ and \bar{p} as a function of collision centrality in Au+Au collisions at $\sqrt{s_{NN}} = 7.7, 11.5, 39, 200$ GeV, respectively.

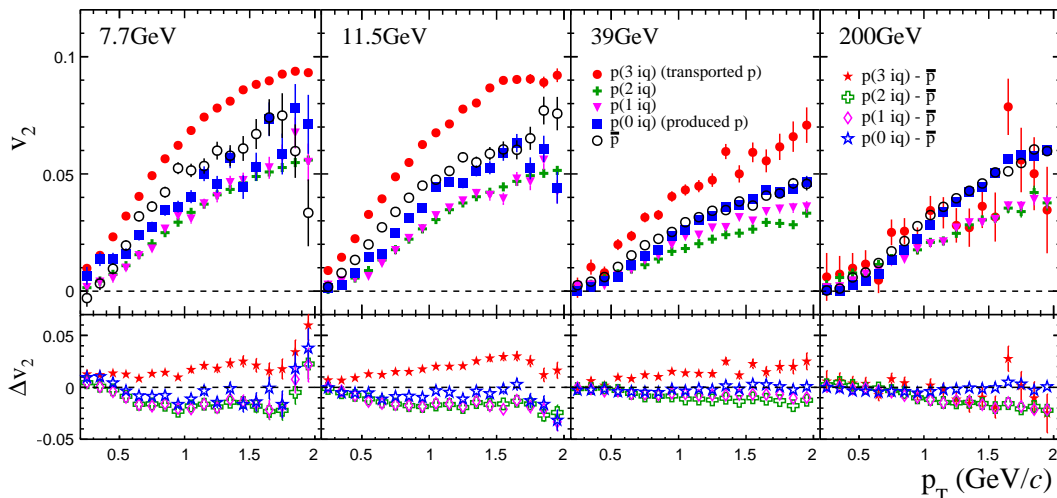


FIG. 2: (Color online) Upper panel: The elliptic flow of $p(3 \text{ iq})$, $p(2 \text{ iq})$, $p(1 \text{ iq})$, $p(0 \text{ iq})$ and \bar{p} as a function of the transverse momentum p_T for 0-80% central Au+Au collisions at $\sqrt{s_{NN}} = 7.7, 11.5, 39, 200$ GeV. The lower panels show the difference of $v_2(p_T)$ between $p(3 \text{ iq})$, $p(2 \text{ iq})$, $p(1 \text{ iq})$, $p(0 \text{ iq})$ and \bar{p} , respectively.

$p(0 \text{ iq})$ and \bar{p} . The v_2 of $p(1 \text{ iq})$ and $p(2 \text{ iq})$ is smaller than that of $p(0 \text{ iq})$ and \bar{p} . Thus, in the UrQMD model, the v_2 of inclusive p is slightly lower than or consistent with the v_2 of \bar{p} depending on the collision energy which is consistent with the results in ref [33].

The upper panel of Figure 2 shows the elliptic flow of $p(3 \text{ iq})$, $p(2 \text{ iq})$, $p(1 \text{ iq})$, $p(0 \text{ iq})$ and \bar{p} as a function of transverse momentum p_T in 0-80% Au+Au collisions at $\sqrt{s_{NN}} = 7.7, 11.5, 39, 200$ GeV. The lower panel shows the difference of v_2 between $p(3 \text{ iq})$, $p(2 \text{ iq})$, $p(1 \text{ iq})$, $p(0 \text{ iq})$ and \bar{p} , respectively. The difference of v_2 between $p(0$

$\text{iq})$ and \bar{p} does not show a clearly p_T dependence and is almost consistent with 0 except 7.7 GeV. But the difference of v_2 between $p(3 \text{ iq})$ and \bar{p} shows a weak p_T dependence. The splitting of v_2 between $p(3 \text{ iq})$ and $p(0 \text{ iq})$ may be due to the stronger flow of transported quarks which experience more interactions than produced quarks. This phenomenon is consistent with the study in ref [22], by assuming the v_2 of transported quarks is larger than that of produced quarks, and it results in a splitting of v_2 between protons and anti-protons. The v_2 of $p(2 \text{ iq})$ and $p(1 \text{ iq})$ increase with p_T , but are systematically smaller

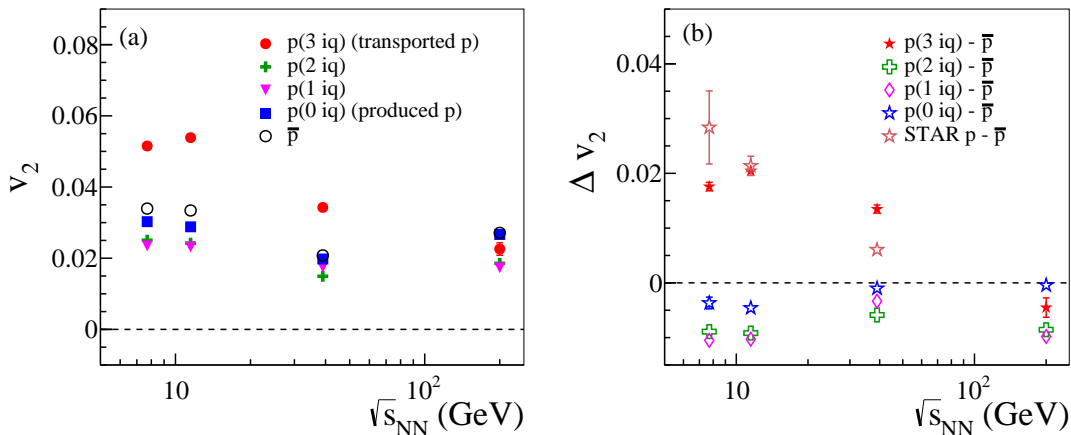


FIG. 3: (Color online) Panel (a): The integrated v_2 of $p(3 \text{ iq})$, $p(2 \text{ iq})$, $p(1 \text{ iq})$, $p(0 \text{ iq})$ and \bar{p} as a function of colliding energy for 0-80% central Au+Au collisions. Panel (b): The difference in v_2 between $p(3 \text{ iq})$, $p(2 \text{ iq})$, $p(1 \text{ iq})$, $p(0 \text{ iq})$ and \bar{p} as a function of colliding energy for 0-80% central Au + Au collisions, respectively.

than that of $p(3 \text{ iq})$, $p(0 \text{ iq})$ and \bar{p} .

To compare with the STAR results, we present the p_T integrated v_2 of $p(3 \text{ iq})$, $p(2 \text{ iq})$, $p(1 \text{ iq})$, $p(0 \text{ iq})$ and \bar{p} within $0.2 < p_T < 2.0 \text{ GeV}/c$ as a function of colliding energy. In Figure 3, panel (a) shows the integrated elliptic flow v_2 of $p(3 \text{ iq})$, $p(2 \text{ iq})$, $p(1 \text{ iq})$, $p(0 \text{ iq})$ and \bar{p} as a function of colliding energy in Au+Au collisions. Panel (b) shows the difference in v_2 from STAR measurements and UrQMD model as a function of colliding energy in Au+Au collisions. The v_2 of $p(3 \text{ iq})$ is systematically larger than that of $p(0 \text{ iq})$ and \bar{p} . Thus the v_2 difference between $p(3 \text{ iq})$ and \bar{p} is larger than 0. The v_2 difference between $p(0 \text{ iq})$ and \bar{p} is slightly smaller than 0 or consistent with 0 depending on the colliding energy. The v_2 of $p(2 \text{ iq})$ and $p(1 \text{ iq})$ are systematically smaller than that of $p(3 \text{ iq})$, $p(0 \text{ iq})$ and \bar{p} . So the difference of v_2 between $p(2 \text{ iq})/p(1 \text{ iq})$ and \bar{p} are smaller than 0. The difference of v_2 between the $p(3 \text{ iq})$ and \bar{p} show a similar energy dependence compared with the STAR results. Our results of $p(3 \text{ iq}) - \bar{p}$ show a good agreement with the STAR results below 11.5 GeV. At 39 GeV, the v_2 difference of $p(3 \text{ iq})$ and \bar{p} are not consistent with the STAR results quantitatively. The yield of $p(3 \text{ iq})$ is relatively smaller than that of $p(2 \text{ iq})$ and $p(1 \text{ iq})$, the v_2 of all protons is much smaller than that in the STAR results. This study indicates that the v_2 difference of STAR measurements may be partly due to the v_2 difference between $p(3 \text{ iq})$ and \bar{p} . But it can not explain the STAR results. In principle, the yield of $p(3 \text{ iq})$ dominates the yield of protons at low energies. The magnitude of v_2 difference of $p(3 \text{ iq}) - \bar{p}$ being consistent between STAR data and UrQMD model in Au+Au collisions at 7.7 and 11.5 GeV suggests that the hadronic interactions are dominant in these collision energies. The derivation of v_2 difference between STAR results and our calculations at 39 GeV indicates that the partonic interactions are also important to build up v_2 at high energies. Additionally, with the energy increas-

ing the fraction of $p(3 \text{ iq})$ relative to inclusive protons decreases can also lead to such a derivation.

V. SUMMARY

In summary, by tracing the number of initial quarks in the UrQMD model, the $p(3 \text{ iq})$, $p(2 \text{ iq})$, $p(1 \text{ iq})$, $p(0 \text{ iq})$ can be distinguished. It provides a way to study the elliptic flow of transported protons and produced protons. We found that the elliptic flow of produced protons shows similar dependence on collision centrality, transverse momentum and colliding energy with anti-protons. The possible explanation is produced protons and anti-protons are both made up of produced quarks. At the same time, the produced protons and anti-protons can be only produced at the early stage in the hadronic evolution of the system. Both of them experience the similar magnitude of interactions in the system which lead to similar v_2 . For the transported protons, the elliptic flow is systematically larger than that of anti-proton as a function of collision centrality, transverse momentum and colliding energy. This can be explained as following: quarks transported from forward rapidity to mid-rapidity by the baryon stopping effect gain larger v_2 than produced quarks. The v_2 of $p(2 \text{ iq})$ and $p(1 \text{ iq})$ are systematically smaller than that of transported protons, produced protons and anti-protons. Our results with the UrQMD model indicate that the splitting of v_2 for protons may partly arise from the difference of v_2 between transported quarks and produced quarks. The difference of v_2 between transported protons with 3 initial quarks and anti-protons show a good quantitative agreement with that between protons and anti-protons in STAR measurements at low energies (7.7 and 11.5 GeV), but large deviation at high energies ($\geq 39 \text{ GeV}$). It suggests the hadronic interactions are domi-

nant in collisions at 7.7 and 11.5 GeV. Without partonic interactions in the UrQMD model, it is problematic to reproduce the v_2 at higher energy (≥ 39 GeV). On the other hand, the fraction of transported protons relative to inclusive protons may also attribute the derivation between STAR data and the UrQMD model.

ACKNOWLEDGMENTS

This work is supported in part by the MoST of China 973-Project No. 2015CB856901, National Natural Science Foundation of China under Grants No. 11890711 and self-determined research funds of CCNU from the colleges basic research and operation of MOE under Grant No. CCNU18TS031.

-
- [1] I. Arsene *et al.* [BRAHMS Collaboration], Nucl. Phys. A **757** (2005) 1
- [2] B. B. Back *et al.* [PHOBOS Collaboration], Nucl. Phys. A **757**, 28 (2005)
- [3] J. Adams *et al.* [STAR Collaboration], Nucl. Phys. A **757**, 102 (2005)
- [4] K. Adcox *et al.* [PHENIX Collaboration], Nucl. Phys. A **757**, 184 (2005)
- [5] K. Aamodt *et al.* [ALICE Collaboration], Phys. Rev. Lett. **105**, 252302 (2010)
- [6] K. Aamodt *et al.* [ALICE Collaboration], Phys. Rev. Lett. **106**, 032301 (2011)
- [7] Z. Q. Feng, Nucl. Sci. Tech. **29**, 40 (2018)
- [8] X. H. Jin, J. H. Chen, Y. G. Ma, S. Zhang, C. J. Zhang and C. Zhong, Nucl. Sci. Tech. **29**, 54 (2018).
- [9] J. Yang and W. N. Zhang, Nucl. Sci. Tech. **27**, 147 (2016).
- [10] X. Luo and N. Xu, Nucl. Sci. Tech. **28**, 112 (2017)
- [11] H. Song, Y. Zhou and K. Gajdosova, Nucl. Sci. Tech. **28**, 99 (2017)
- [12] J. Y. Ollitrault, Phys. Rev. D **46**, 229 (1992).
- [13] H. Sorge, Phys. Rev. Lett. **78**, 2309 (1997)
- [14] H. Sorge, Phys. Rev. Lett. **82**, 2048 (1999)
- [15] C. M. Ko and F. Li, Nucl. Sci. Tech. **27**, no. 6, 140 (2016). doi:10.1007/s41365-016-0141-3
- [16] Z. Y. Lu, G. X. Peng, S. P. Zhang, M. Ruggieri and V. Greco, Nucl. Sci. Tech. **27**, 148 (2016).
- [17] L. Adamczyk *et al.* [STAR Collaboration], Phys. Rev. Lett. **110**, no. 14, 142301 (2013)
- [18] L. Adamczyk *et al.* [STAR Collaboration], Phys. Rev. C **88**, 014902 (2013)
- [19] L. Adamczyk *et al.* [STAR Collaboration], Phys. Rev. C **86**, 054908 (2012)
- [20] L. Adamczyk *et al.* [STAR Collaboration], Phys. Rev. C **93**, 014907 (2016)
- [21] Shusu Shi, Adv. High Energy Phys. **2016**, 1987432 (2016)
- [22] J. C. Dunlop, M. A. Lisa and P. Sorensen, Phys. Rev. C **84**, 044914 (2011)
- [23] P. C. Li, Y. J. Wang, Q. F. Li and H. F. Zhang, Nucl. Sci. Tech. **29**, 177 (2018).
- [24] Y. Burnier, D. E. Kharzeev, J. Liao and H. U. Yee, Phys. Rev. Lett. **107**, 052303 (2011)
- [25] J. Xu, T. Song, C. M. Ko and F. Li, Phys. Rev. Lett. **112**, 012301 (2014)
- [26] C. M. Ko, T. Song, F. Li, V. Greco and S. Plumari, Nucl. Phys. A **928**, 234 (2014)
- [27] J. Xu, L. W. Chen, C. M. Ko and Z. W. Lin, Phys. Rev. C **85**, 041901 (2012)
- [28] M. Bleicher *et al.*, J. Phys. G **25**, 1859 (1999)
- [29] S. A. Bass *et al.*, Prog. Part. Nucl. Phys. **41**, 255 (1998)
- [30] S. Voloshin and Y. Zhang, Z. Phys. C **70**, 665 (1996)
- [31] A. M. Poskanzer and S. A. Voloshin, Phys. Rev. C **58**, 1671 (1998)
- [32] Y. Guo, F. Liu and A. Tang, Phys. Rev. C **86**, 044901 (2012)
- [33] Q. Li, Y. Wang, X. Wang and C. Shen, Sci. China Phys. Mech. Astron. **59**, 632001 (2016)